

# 1 **Rainfall threshold calculation for debris flow early** 2 **warning in areas with scarcity of data**

3 **Hua-li Pan**<sup>1, 2</sup>, **Yuan-jun Jiang**<sup>1, 2, ✉</sup>, **Jun Wang**<sup>3</sup>, **Guo-qiang Ou**<sup>1, 2</sup>

4 ✉ Corresponding author's e-mail: yuanjun.jiang.civil@gmail.com

5 <sup>1</sup> Key Laboratory of Mountain Hazards and Earth Surface Process, Chinese Academy of Sciences, Chengdu  
6 610041, China

7 <sup>2</sup> Institute of Mountain Hazards and Environment, Chinese Academy of Sciences, Chengdu 610041, China

8 <sup>3</sup> Guangzhou Institute of Geography, Guangzhou 510070, China

9 **Abstract:** Debris flows are one of the natural disasters that frequently occur in mountain ar-  
10 eas, usually accompanied by serious loss of lives and properties. One of the most used ap-  
11 proaches to mitigate the risk associated to debris flows is the implementation of early warning  
12 systems based on well calibrated rainfall thresholds. However, many mountainous areas have  
13 little data regarding rainfall and hazards, especially in debris flow forming regions. Therefore,  
14 the traditional statistical analysis method that determines the empirical relationship between  
15 rainstorm and debris flow events cannot be effectively used to calculate reliable rainfall  
16 threshold in these areas. After the severe Wenchuan earthquake, there were plenty of materi-  
17 als deposited in the gullies which resulted in lots of debris flow events subsequently. The trig-  
18 gering rainfall threshold has decreased obviously. To get a reliable and accurate rainfall  
19 threshold and improve the accuracy of debris flow early warning, this paper developed a  
20 quantitative method, which is suit for debris flow triggering mechanism in meizoseismal areas,  
21 to identify rainfall threshold for debris flow early warning in areas with scarcity of data based  
22 on the initiation mechanism of hydraulic-driven debris flow. First, we studied the characteris-  
23 tics of the study area, including meteorology, hydrology, topography and physical characteris-  
24 tics of the loose solid materials. Then, the rainfall threshold was calculated by the initiation  
25 mechanism of the hydraulic debris flow. The results show that the proposed rainfall threshold  
26 curve is a function of the antecedent precipitation index and 1-h rainfall. To test the proposed

27 method, we selected the Guojuanyan gully, a typical debris flow valley that during the  
28 2008-2013 period experienced several debris flow events and that is located in the meizo-  
29 seismic areas of Wenchuan earthquake, as a case study. We compared the calculated thresh-  
30 old with observation data, showing that the accuracy of the method is satisfying and thus can  
31 be used for debris flow early warning in areas with scarcity of data.

32 **Keywords:** Debris flow; rainfall threshold curve; rainfall threshold; areas with scarcity of  
33 data

## 34 **1 Introduction**

35 Debris flow is rapid, gravity-induced mass movement consisting of a mixture of water,  
36 sediment, wood and anthropogenic debris that propagate along channels incised on mountain  
37 slopes and onto debris fans (Gregoretti et al., 2016). It has been reported in over 70 countries  
38 in the world and often causes severe economic losses and human casualties, seriously  
39 retarding social and economic development (Imaizumi et al., 2006; Tecca and Genevois, 2009;  
40 Dahal et al., 2009; Liu et al., 2010; Cui et al., 2011; McCoy et al., 2012; Degetto et al., 2015;  
41 Tiranti and Deangeli, 2015; Hu et al., 2016). Rainfall is an important component of debris  
42 flows and is the most active factor when debris flows occur, which also determines the  
43 temporal and spatial distribution characteristics of the hazards. As one of the important and  
44 effective means of non-engineering disaster mitigation, much attention has been paid to  
45 debris flow early warning by researchers (Pan et al., 2013; Guo et al., 2013; Zhou et al., 2014;  
46 Wei et al., 2017). For rainstorm debris flows, the precipitation and intensity of rainfall are the  
47 decisive factors of debris flow initiation, and a reasonable rainfall threshold target is essential  
48 to ensuring the accuracy of debris flow early warning. However, if there are some extreme  
49 events occurred, such as an earthquake, the rainfall threshold of debris flow may change a lot.  
50 Take the main earthquake-hit areas affected by the Wenchuan earthquake for example. In the  
51 several years since the earthquake, intensive rainfall events have triggered massive debris  
52 flows resulting in serious casualties and property loss, even in some of the gullies which have  
53 never had debris flow before. For example, the Guojuanyang gully, a small gully located in the  
54 meizoseismic areas of the big earthquake, has no debris flows under the annual average  
55 rainfall before 2008, but it became a debris flow gully after the earthquake under the same

56 conditions, even the rainfall was smaller than the annual average rainfall. This indicates that  
57 earthquakes have a big influence on debris flow occurrence. The earthquake triggered many  
58 unstable slopes, collapses, and landslides, which have served as the source material for  
59 debris flow and shallow landslide in the years after the earthquake (Tang et al. 2009, 2012; Xu  
60 et al. 2012; Hu et al. 2014). Therefore, the rainfall threshold of debris flow post-earthquake  
61 is an important and urgent issue to study for debris flow early warning and mitigation.

62 As an important and effective means of disaster mitigation, debris flow early warning  
63 have received much attention from researchers. The rainfall threshold is the core of the debris  
64 flow early warning, on which have a great deal of researches yet (Cannon et al., 2008; Chen  
65 and Huang 2010; Baum and Godt, 2010; Staley et al., 2013; Winter et al., 2013; Zhou and Tang,  
66 2014; Segoni et al., 2015; Rosi et al 2015). Although the formation mechanism of debris flow  
67 has been extensively studied, it is difficult to perform distributed physically based modeling  
68 over large areas, mainly because the spatial variability of geotechnical parameters is very  
69 difficult to assess (Tofani et al., 2017). Therefore, many researchers (Wilson and Joyko, 1997;  
70 Campbell, 1975; Cheng et al., 1998) have had to determine the empirical relationship between  
71 rainfall and debris flow events and to determine the rainfall threshold depending on the  
72 combinations of rainfall parameters, such as antecedent rainfall, rainfall intensity, cumulative  
73 rainfall, et al.. Takahashi (1978), Iverson (1989) and Cui (1991) predicted the formation of  
74 debris flow based on studies of slope stability, hydrodynamic action and the influence of pore  
75 water pressure on the formation process of debris flow. Caine (1980) first statistically  
76 analyzed the empirical relationship between rainfall intensity and the duration of debris flows  
77 and shallow landslides and proposed an exponential expression ( $I = 14.82D^{-0.39}$ ). Afterwards,  
78 other researchers, such as Wieczorek (1987), Jison (1989), Hong et al. (2005), Dahal and  
79 Hasegawa (2008), Guzzetti et al. (2008) and Saito et al. (2010), carried out further research  
80 on the empirical relationship between rainfall intensity and the duration of debris flows,  
81 established the empirical expression of rainfall intensity - duration ( $I = D$ ) and proposed  
82 debris flow prediction models. Shied and Chen (1995) established the critical condition of  
83 debris flow based on the relationship between cumulative rainfall and rainfall intensity. Zhang  
84 (2014) developed a model for debris flow forecasting based on the water-soil coupling  
85 mechanism at the watershed scale. Tang et al. (2012) analyzed the critical rainfall of Beichuan

86 city and found that the cumulative rainfall triggering debris flow decreased by 14.8%-22.1%  
87 when compared with the pre-earthquake period, and the critical hour rainfall decreased by  
88 25.4%-31.6%. Chen et al. (2013) analyzed the pre- and post-earthquake critical rainfall for  
89 debris flow of Xiaogangjian gully and found that the critical rainfall for debris flow in 2011 was  
90 approximately 23% lower than the value during the pre-earthquake period. Other researches,  
91 such as Chen et al. (2008) and Shied et al. (2009) has reached similar conclusions that the  
92 post-earthquake critical rainfall for debris flow is markedly lower than that of the  
93 pre-earthquake period. Zhenlei Wei et al. (2017) investigated a rainfall threshold method for  
94 predicting the initiation of channelized debris flows in a small catchment, using field  
95 measurements of rainfall and runoff data.

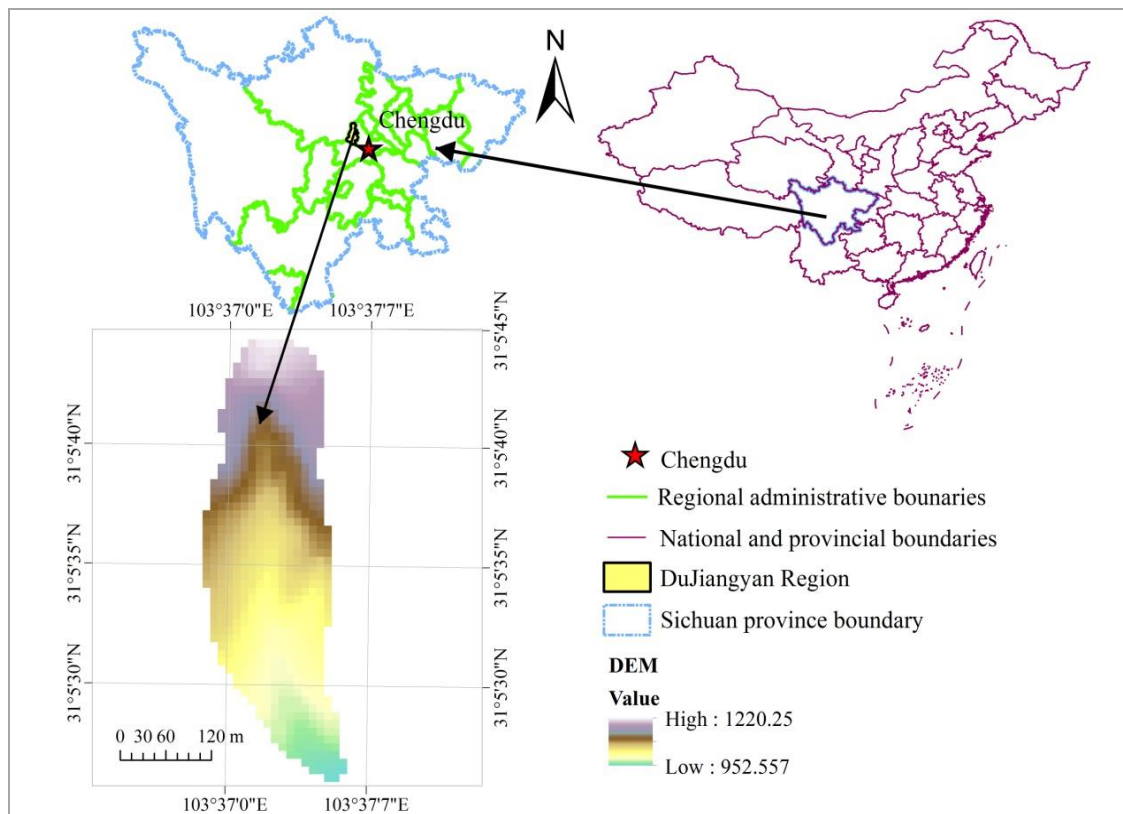
96 Overall, the studies on the rainfall threshold of debris flow can be summarized as two  
97 methods: the demonstration method and the frequency calculated method. The  
98 demonstration method employs statistical analysis of rainfall and debris flow data to study the  
99 relationship between rainfall and debris flow events and to obtain the rainfall threshold curve  
100 (Bai et al., 2008; Tian et al., 2008; Zhuang, et al., 2009). The I-D approaches would be this  
101 kind of method. This method is relatively accurate, but it needs very rich, long-term rainfall  
102 sequence data and disaster information; therefore, it can be applied only to areas with a  
103 history of long-term observations, such as Jiangjiagou, Yunnan, China, and Yakedake, Japan.  
104 The frequency calculated method, assuming that debris flow and torrential rain have the same  
105 frequency, and thus, debris flow rainfall threshold can be calculated based on the rainstorm  
106 frequency in the mountain towns where have abundant rainfall data but lack of disaster data  
107 (Yao, 1988; Liang and Yao, 2008). Researchers have also analyzed the relationship between  
108 debris flow occurrences and precipitation and soil moisture content based on initial debris  
109 flow conditions (Hu and Wang, 2003). However, this approach is rarely applied to the  
110 determination of debris flow rainfall thresholds because it needs series of rainfall data. Pan et  
111 al. (2013) calculated the threshold rainfall for debris flow pre-warning by calculating the  
112 critical depth of debrisflow initiation combined with the amount and regulating factors of  
113 runoff generation.

114 Most mountainous areas have little data regarding rainfall and hazards, especially in  
115 Western China. When a debris flow outbreak occurs, it often causes serious harm to villages,

116 farmland, transport centers and water conservation facilities in the downstream area. Neither  
117 the traditional demonstration method nor frequency calculated method can satisfy the debris  
118 flow early warning requirements in these areas. Therefore, how to calculate the rainfall  
119 threshold in these data-poor areas has become one of the most important challenges for the  
120 debris flow early warning systems. To solve this problem, this paper developed a quantitative  
121 method of calculating rainfall threshold for debris flow early warning in areas with scarcity of  
122 data based on the initiation mechanism of hydraulic-driven debris flows.

## 123 2 Study site

### 124 2.1 Location and gully characteristics of the study area



125

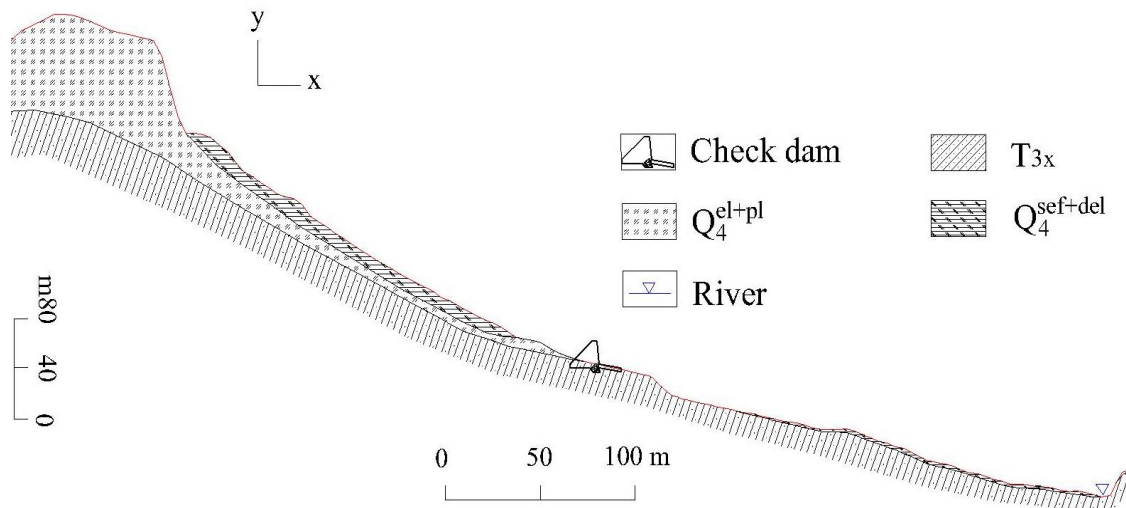
126

**Figure 1.** The location of the Guojuanyan gully

127 The Guojuanyan gully in Du Jiangyan city, located in the meizoseismal areas of the  
128 Wenchuan earthquake, China, was selected as the study area (Fig. 1). It is located at the  
129 Baisha River, which is the first tributary of the Minjiang River. The seismic intensity of the  
130 study area was XI, which was the maximum seismic intensity of the Wenchuan earthquake.

131 The Shenxi Gully Earthquake Site Park is at the right side of this gully. The area extends from  
 132  $31^{\circ}05'27''$  N to  $31^{\circ}05'46''$  N latitude and  $103^{\circ}36'58''$  E to  $103^{\circ}37'09''$  E longitude, covering an  
 133 area of  $0.15 \text{ km}^2$  with a population of 20 inhabitants. The elevation range is from 943 m to  
 134 1222 m, the average gradient of the main channel is 270‰ (the average slope angle is  $15.1^{\circ}$ ),  
 135 and the length of the main channel is approximately 580m.

136 Geologically, the Guojuanyan gully is composed of bedrock and Quaternary strata. The  
 137 bedrock is upper Triassic Xujiahe petrofabric ( $T_{3x}$ ) whose lithology is mainly sandstone;  
 138 mudstone; carbonaceous shale belonging to layered, massive structures; and semi solid-solid  
 139 petrofabric. The Quaternary strata are alluvium ( $Q_4^{el+pl}$ ), alluvial materials ( $Q_4^{pl+dl}$ ), landslide  
 140 accumulations and debris flow deposits ( $Q_4^{sef+del}$ ). The thickness of the Quaternary strata  
 141 ranges from 1 m to 20 m and varies greatly. The strata profile of the Guojuanyan gully is  
 142 shown in Fig. 2.



143  
 144 **Figure 2.** The strata profile of the Guojuanyan gully (Jun Wang et al, 2017)

145 Geomorphologically, the study area belongs to the Longmenshan Mountains. The famous  
 146 Longmenshan tectonic belt has a significant effect on this region, especially the Hongkou-  
 147 Yinxiu fault. The study area has strong tectonic movement and strong erosion, and the main  
 148 channel is “V”-shaped. The area is characterized by a rugged topography, and the main slope  
 149 gradient interval of the gully is  $20^{\circ}$  to  $40^{\circ}$ , accounting for 52.38% of the entire study area.

150 Climatically, this area has a subtropical and humid climate, with an average annual  
 151 temperature of  $15.2^{\circ}\text{C}$  and an average annual rainfall of 1200 mm (Wang et al., 2014).

152 **2.2 Materials and debris flow characteristics of the study area**

153 The Wenchuan earthquake generated a landslide in the Guojuanyan gully, leading to an  
 154 abundance of loose deposits that have served as the source materials for debris flows. A com-  
 155 parison of the Guojuanyan gully before and after the Wenchuan earthquake is shown in Fig. 3.  
 156 According to the field investigation and field tests, the landslide 3D characteristics induced by  
 157 the earthquake and the infiltration characteristics of the loose materials are shown in Table 1  
 158 and Table 2 (Wang et al., 2016). They indicate that the volume of materials is more than  $20 \times$   
 159  $10^4 \text{ m}^3$ , and the infiltration capable of the earth surface have much increased. Therefore, the  
 160 trigger rainfall for debris flow has decreased greatly. The Guojuanyan gully had no debris  
 161 flows before the earthquake because of the lack of loose solid materials before the earthquake;  
 162 however, it became a debris flow gully after the earthquake, and debris flows occurred in the  
 163 following years (Table 3). The specific conditions of these debris flow events were collected  
 164 through field investigations and interviews. The field investigations and experiments deter-  
 165 mined that the density of the debris flow was between 1.8 and 2.1 g/cm<sup>3</sup>. Unfortunately, there  
 166 were no rainfall data before 2011, when we started field surveys in the Guojuanyan gully.



167  
 168 (a) 14 September, 2006 (b) 28 June, 2008

169 **Figure 3.** The Guojuanyan gully before (a) and after the Wenchuan earthquake (b) (from Google Earth)

170 **Table 1.** The landslide 3D characteristics induced by the earthquake in the study area

Average length /m	Average width /m	Average Height /m	Average depth /m	Slope /°	Volume / $\times 10^4 \text{ m}^3$
160	80	180	15	$\geq 30$	20

171

172 **Table 2.** The infiltration characteristics of solid materials in the study area

Infiltration curve	Infiltration rate	
	Initial infiltration /cm/min	Stable infiltration /cm/min
$f = 0.6529 \cdot \exp(-0.057 \cdot t)$	3.52	0.34

173 **Table 3.** The specific conditions of debris flow events in the Guojuanyan gully after the earthquake

Time	Volume (10 <sup>4</sup> m <sup>3</sup> )	Surges	Rainfall data record
24 September, 2008	0.6	1	No
17 July, 2009	0.8	1	No
13 August, 2010	4.0	3	No
17 August, 2010	0.4	1	No
1 July, 2011	0.8	1	Yes
17 August, 2012	0.7	1	Yes
9 July, 2013	0.4	1	Yes
26 July, 2013	2.0	2	Yes
18 July, 2014	1.5	1	Yes

174

### 175 **2.3 Debris flow monitoring and streambed survey of the study area**

176 After the Wenchuan earthquake, continuous field surveillance was undertaken in the  
 177 study area. A debris flow monitoring system was also established in the study area. To identify  
 178 the debris flow events, this monitoring system recorded stream water depth, precipitation and  
 179 real-time video of the gully (Fig. 4). The water depth was measured using an ultrasonic level  
 180 meter, and precipitation was recorded by a self-registering rain gauge. The real-time video  
 181 was recorded onto a data logger and transmitted to the monitoring center, located in the In-  
 182 stitute of Mountain Hazards and Environment, Chinese Academy of Sciences. When a rain-  
 183 storm or a debris flow event occurs, the realtime data, including rainfall data, video record,  
 184 and water depth data, can be observed and queried directly in the remote client computer in  
 185 the monitoring center. Fig. 5 shows images taken from the recorded video. These data can be  
 186 used to analyze the rainfall or other characteristics, such as the 10-min, 1- and 24-h critical  
 187 rainfall. The recorded video is usually used to analyse the whole inundated process of debris  
 188 flow events and to identify debris flow events as well as the data from rainfall, flow depth, and  
 189 field investigation.





(a) Real-time camera and rain gauge (b) Ultrasonic level meters

**Figure 4.** Debris flow monitoring system in the study area

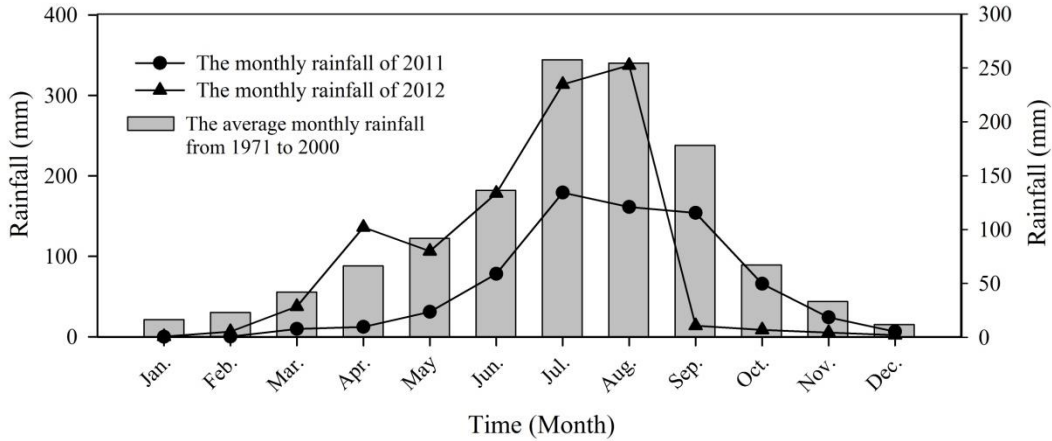


**Figure 5.** Real-time images from video taken during the debris flow movement

## 2.4 Data collection and the characteristics of rainfall

The Wenchuan earthquake occurred in the Longmenshan tectonic belt, located on the eastern edge of the Tibetan plateau, China, which is one of three rainstorm areas of Sichuan Province (Longmen mountain rainstorm area, Qingyi river rainstorm area and Daba mountain rainstorm area). Heavy rainstorms and extreme rainfall events occur frequently. Because there were few data in the mountain areas, we collected the rainfall data from 1971- 2000 and 2011-2012 (from our own on-site monitoring); the characteristics of the rainfalls are as following:

(1) Abundant precipitation: The average annual precipitation was 1177.3 mm from 1971 to 2000, and the average monthly precipitation is shown in Fig. 6. From 1971 to 2000, the minimum annual precipitation of 713.5 mm occurred in 1974, and the maximum annual precipitation of 1605.4 mm occurred in 1978. The total precipitation in 2012 is 1148mm, in the trend range of the historical data.

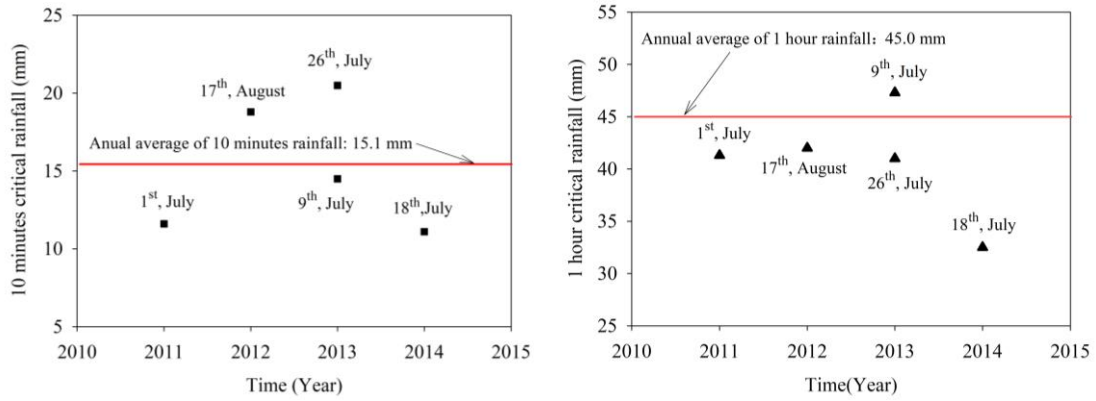


208  
 209 **Figure 6.** The average monthly precipitation of the Guojuanyan gully from 1971 to 2000 and the  
 210 monthly rainfall of 2011 and 2012

211 (2) Severely inhomogeneous distribution of precipitation in time: from Fig. 6 we can ob-  
 212 serve that rainfall is seasonal, with approximately 80% of the total rainfall occurring during  
 213 the monsoon season (from June to September) and the other 20% in other seasons. And the  
 214 laws of monthly rainfall in 2011 and 2012 coincide to the historical data. For instance, in 2012,  
 215 the total annual rainfall in this area was approximately 1148 mm, and rainfall in the monsoon  
 216 season from June to September was 961 mm, accounting for 83.7% of the annual total.

217 (3) Due to the impact of the atmospheric environment, the regional and annual distribu-  
 218 tion of rainfall is seriously inhomogeneous; moreover, the rainfall intensity has great differ-  
 219 ences. From 1971 to 2000, the maximum monthly rainfall was 592.9 mm, the daily maximum  
 220 rainfall was 233.8 mm, the hourly maximum rainfall was 83.9 mm, the 10-min maximum  
 221 rainfall was 28.3 mm, and the longest continuous rainfall time was 28 days.

222 Debris flow field monitoring data and on-site investigation data were used to identify the  
 223 debris flow events and to analyze the characteristics of the rainfall pattern and the critical  
 224 rainfall characteristics. Analysing the typical rainfall process curves (Fig. 13), we can find that  
 225 the hourly rainfall pattern of the Guojuanyan gully is the peak pattern, displaying the single  
 226 peak and multippeak, a characteristic of short-duration rainstorms. Through the statistical  
 227 analysis of the 10-min, 1-, and 24-h critical rainfall of debris flow events after the earthquake,  
 228 their characteristics can be obtained, as shown in Fig. 7.

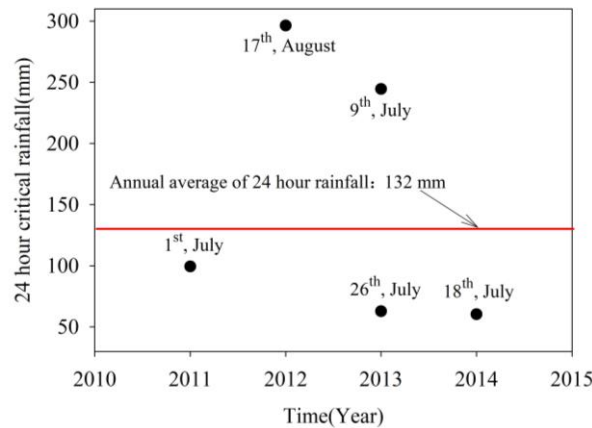


229

230

(a) The 10-min critical rainfall

(b) The 1-h critical rainfall



231

232

(c) The 24-h critical rainfall

233

**Figure 7.** The critical rainfall of debris flows in the Guojuanyan gully

234

Fig. 7a shows that the observed 10-min critical rainfall is between 11.1 mm and 21.5 mm.

235

According to the Sichuan Hydrology Record Handbook (Sichuan Water and Power Department

236

1984), the annual average of maximum 10-min rainfall of the study area is approxi-

237

mately 15.1 mm (from 1940-1975). According to the observation, 60% of debris flow events

238

occurred below the annual average 10-min rainfall. In addition, the 1-h critical rainfall varied

239

between 34.5 mm and 47.3 mm in the study area (Fig. 7b). And the annual average of maxi-

240

mum 1-h rainfall is 45.0 mm (from 1940-1975) based on the Sichuan Hydrology Record

241

Handbook (Sichuan Water and Power Department 1984). Figure 10b shows that 80% debris

242

flow events occurred below the annual average 1-h rainfall, except for the debris flow event

243

occurred on July 9, 2013. At last, the minimum value of 24-h critical rainfall is 60.4 mm and

244

the maximum value is 296.4 mm in the study area. According to the Sichuan Hydrology Rec-

245

ord Handbook (Sichuan Water and Power Department 1984), the annual average of maxi-

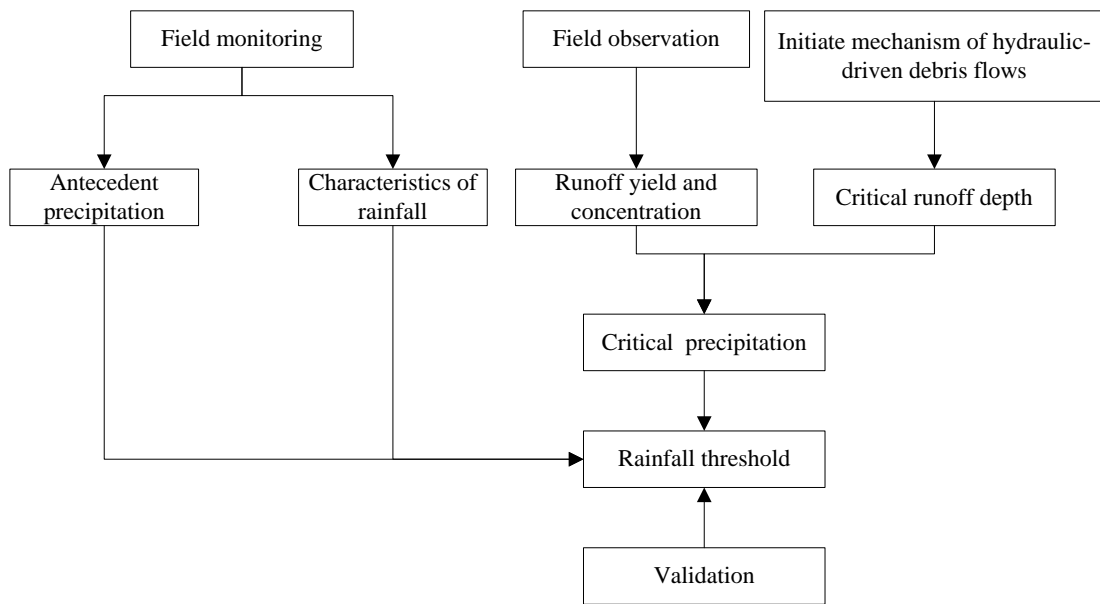
246 mum 24-h rainfall is 132 mm (from 1940-1975). From Fig. 7c, we can see that 24-h critical  
247 rainfall for different debris flow events vary widely and 60% debris flow events occurred be-  
248 low the annual average 24-h rainfall.

249 From the above study, we can find that the 10-min and the 1-h critical rainfalls of  
250 different debris flow events have minor differences; however, the 24-h critical rainfalls vary  
251 widely. The reason is that debris flow is usually triggered by short-duration rainstorms.  
252 Therefore, the short-durations of 10-min and 1-h rainfall have higher correlation with debris  
253 flow occurrence and have the minor differences. **Actually, the 10-min rainfall intensity**  
254 **(maximum precipitation over a 10-min period during the rainfall event) is the most**  
255 **appropriate index for early warning of debris flow, which is most representative and has**  
256 **minor error. However, it is difficult to obtain such short-duration rainfall data in actual debris**  
257 **flow gullies because long-term rainfall monitoring system do not exist in most debris flow**  
258 **basins especially in areas with scarcity of data.** Further analyzing the 10-min and 1-h critical  
259 rainfalls, we can find that they vary with the antecedent precipitation index ( *API* ). They are  
260 variable rather than constant. In this paper, the antecedent precipitation index ( *API* ) and the  
261 1-h rainfall (  $I_{60}$  ) were used to calculate the rainfall threshold curve of debris flows in the  
262 Guojuanyan gully.

### 263 **3 Materials and methods**

264 This study makes an attempt to analyze the trigger rainfall threshold for debris flow by  
265 using the initiation mechanism of debris flow. Firstly, to analyze the rainfall characteristics of  
266 the watershed by using the field monitoring data; then to calculate the runoff yield and con-  
267 centration progress based on field observation. Additionally, the critical runoff depth to initi-  
268 ate debris flow was calculated by the initiation mechanism with the underlying surface condi-  
269 tion (materials, longitudinal slope, etc.) of the gully. Then, the corresponding rainfall for the  
270 initiation of debris was back-calculated based on the stored- full runoff generation. At last,  
271 these factors were combined to build the rainfall threshold model. This method can be applied  
272 to the early warning system in the areas with scarcity of rainfall data.

273 The flow chart of the research is shown in Fig. 8.



274  
275

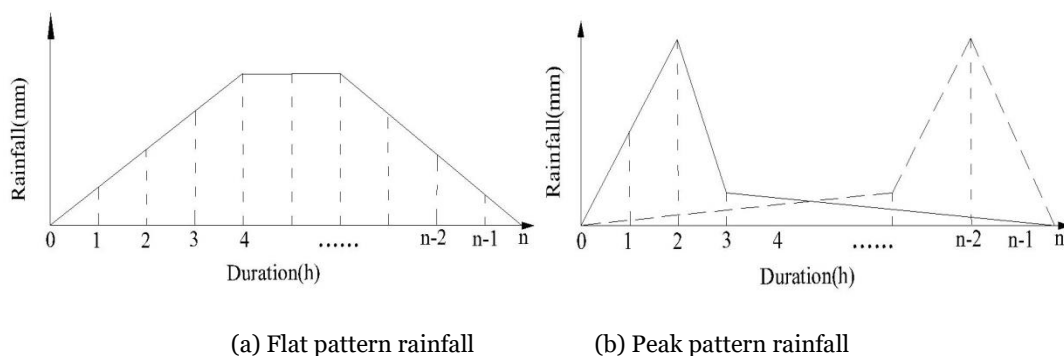
276 **Figure 8.** The flow chart of the research

277 **The main influence factors for the formation of debris flow event include three parts: a**  
 278 **steep longitudinal slope of the gully (served as potential energy condition), abundant solid**  
 279 **materials (source condition) and water source condition (usually is rainfall condition for**  
 280 **rainstorm debris flow).** For rainstorm debris flow events, the precipitation and intensity of  
 281 rainfall are the decisive factors of debris flow initiation. Where if there is no earthquakes or  
 282 other extreme events, the topography of the gully can be considered relatively stable. In  
 283 contrast, rainfall conditions and the distribution of solid materials that determine the  
 284 occurrence of debris flows can display temporal and spatial variation within the same  
 285 watershed. Therefore, it is common to provide warning of debris flows based rainfall data  
 286 after assessing the supply and distribution of loose solid materials. In Takahashi's model, the  
 287 characteristics of soil, such as the porosity and the hydraulic conductivity of soils, are not  
 288 considered, and considered the characteristic particle size and the volume concentration of  
 289 sediment; while the characteristics of topography is mainly represented by the longitudinal  
 290 slope of the gully. **Furthermore, in the stored-full runoff model, the maximum storage**  
 291 **capacity of watershed, which mainly decided by the porosity and permeability of the soil, may**  
 292 **represent the characteristic of the hydraulic conductivity of solid material to a certain extent.**  
 293 Therefore, this study wouldn't consider the hydraulic conductivity any more.

294 **3.1 Rainfall pattern and the spatial-temporal distribution characteristics**

295 Mountain hazards such as debris flows are closely related to rainfall duration, rainfall  
 296 amount and rainfall pattern (Liu et al., 2009). Rainfall pattern not only affects the formation  
 297 of surface runoff but also affects the formation and development of debris flows. Different  
 298 rainfall patterns result in different soil water contents; thus, the internal structure of the soil,  
 299 stress conditions, shear resistance, slip resistance and removable thickness can vary. The ini-  
 300 tiation of a debris flow is the result of both short-duration heavy rains and the antecedent  
 301 rainfall (Cui et al., 2007; Guo et al., 2013). Many previous observational data have shown that  
 302 the initiation of a debris flow often appears at a certain time that has a high correlation with  
 303 the rainfall pattern (Rianna et al., 2014; Mohamad Ayob Mohamadi, 2015).

304 The precipitation characteristics not only affect the formation of runoff, also affect the  
 305 formation and development of the debris flow. Different rainfalls result in different soil water  
 306 contents, and thus the internal structure of the soil, stress conditions, corrosion resistance  
 307 and slip resistance can vary (Pan et al., 2013). Based on the rainfall characteristics, rainfall  
 308 patterns can be roughly divided into two kinds, the flat pattern and the peak pattern, as shown  
 309 in Fig. 9. If the rainfall intensity has little variation, there is no obvious peak in the whole  
 310 rainfall process; such rainfall can be described as flat pattern rainfall. If the soils characterized  
 311 by low hydraulic conductivity, this kind of rainfall no longer time spans are relevant for mass  
 312 movements. And the debris flows, if occur, are mainly caused by the great amount of effective  
 313 antecedent precipitation. While if the rainfall intensity increases suddenly during a certain  
 314 period of time, the rainfall process will have an obvious peak and is termed peak pattern rain-  
 315 fall. If the hydraulic conductivity is high enough, the rainfall can totally enter the soil and  
 316 mass can move easily. These debris flows are mainly controlled by the short-duration heavy  
 317 rains. Peak pattern rainfall may have one peak or multi-peak (Pan, et al., 2013).



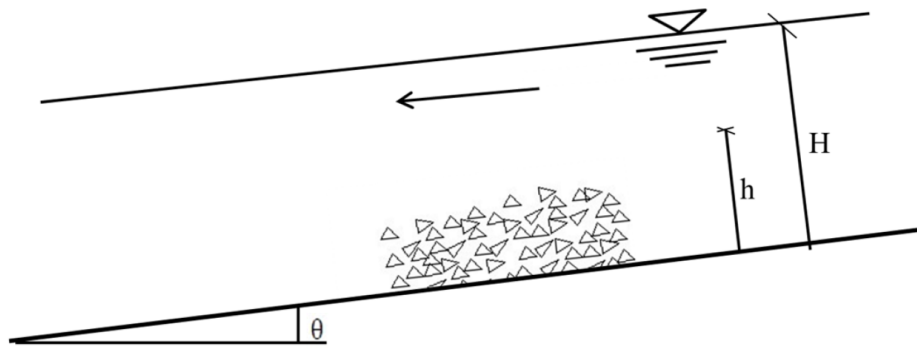
320 **Figure 9.** The diagram of rainfall patterns

321 Through analyzing the rainfall data of the Guojuanyan gully, the rainfall pattern and the  
 322 spatial-temporal distribution characteristics can be obtained.

### 323 3.2 The rainfall threshold curve of debris flows

#### 324 3.2.1 The initiation mechanism of hydraulic-driven debris flows

325 When the watershed hydrodynamics, which include the runoff, soil moisture content and  
 326 the discharge, reach to a certain level, the loose deposits in the channel bed will initiate  
 327 movement and the sediment concentration of the flow will increase, leading the sediment  
 328 laden flow to transform into a debris flow. The formation of this kind of debris flow is a com-  
 329 pletely hydrodynamic process. Therefore, it can be regarded as the initiation problem of de-  
 330bris flow under hydrodynamic force. The forming process of hydraulic-driven debris flows is  
 331 shown in Fig. 10.



332  
 333 **Figure 10.** The typical debris flow initiate model

334 According to Takahashi's model, the critical depth for hydraulic-driven debris flows is:

$$335 \quad h_0 = \left[ \frac{C_* (\sigma - \rho) \tan \phi}{\rho \tan \theta} - \frac{C_* (\sigma - \rho)}{\rho} - 1 \right] d_m \quad (1)$$

336 where  $C_*$  is the volume concentration obtained by experiments(0.812);  $\sigma$  is the unit weight of  
 337 loose deposits (usually is 2.65 g/cm<sup>3</sup>);  $\rho$  is the unit weight of water,1.0 g/cm<sup>3</sup>;  $\theta$  is the longi-  
 338 tudinal slope of the channel (°);  $\phi$  is the internal friction angle (°) and can be measured by  
 339 shear tests ; And  $d_m$  is the average grain diameter (mm), which can be expressed as:

$$340 \quad d_m = \frac{d_{16} + d_{50} + d_{84}}{3} \quad (2)$$



341 where  $d_{16}$ ,  $d_{50}$  and  $d_{84}$  are characteristic particle sizes of the loose deposits (mm), whose  
342 weight percentage are 16%, 50% and 84% separately.

343 Takahashi's model became one of the most common for the initiation of debris flow after  
344 it was presented. A great deal of related studies was published based on Takahashi's model  
345 later. Some discussed the laws of debris flow according to the geomorphology and the water  
346 content while others examined the critical conditions of debris flow with mechanical stability  
347 analysis. However, Takahashi's relation was determined for debris flow propagating over a  
348 rigid bed, hence, with a minor effect of quasi-static actions near the bed. Lanzoni et al. (2017)  
349 slightly modified the Takahashi's formulation of the bulk concentration, which considered the  
350 long-lasting grain interactions at the boundary between the upper, grain inertial layer and the  
351 underlying static sediment bed, and validated the proposed formulation with a wide dataset of  
352 experimental data (Takahashi, 1978, Tsubaki et al., 1983, Lanzoni, 1993, Armanini et al.,  
353 2005). The effects of flow rheology on the basis of velocity profiles are analyzed with attention  
354 to the role of different stress-generating mechanisms.

355 This study aims to the initiation of loose solid materials in the gully under surface runoff;  
356 the interactions on the boundary are not involved. Therefore, Takahashi's model can be used  
357 in this study.

### 358 **3.2.2 Calculation of watershed runoff yield and concentration**

359 The stored-full runoff, one of the modes of runoff production, is also called as the super  
360 storage runoff. The reason of the runoff yield is that the aeration zone and the saturation zone  
361 of the soil are saturated by rainfall. In the humid and semi humid areas where rainfall is  
362 plentiful, because of the high groundwater level and soil moisture content, the loss of precipi-  
363 tation is no longer increased with the rains continue, after meet plant interception and infil-  
364 tration, which produces a wide range of surface runoff. The Guojuanyan gully is located in Du  
365 Jiangyan city, which is in a humid area. Therefore, stored-full runoff is the main pattern run-  
366 off producing mechanism in this gully, and this runoff yield pattern is used to calculate the  
367 watershed runoff. That is, it is supposed that the water storage can reach the maximum stor-  
368 age capacity of the watershed after each heavy rain. It is common used in the humid and semi  
369 humid areas in China to analyze the runoff yield mechanism. Therefore, the rainfall loss in



370 each time  $I$  is the difference between the maximum water storage capacity  $I_m$  and the soil  
 371 moisture content before the rain  $P_a$ . Hence, the water balance equation of stored-full runoff is  
 372 expressed as follows (Ye, et al., 1992):

$$373 \quad R = P - I = P - (I_m - P_a) \quad (3)$$

374 where  $R$  is the runoff depth (mm);  $P$  is the precipitation of one rainfall (mm);  $I$  is the rain-  
 375 fall loss (mm);  $I_m$  is the watershed maximum storage capacity (mm) for a certain watershed,  
 376 it is a constant for a certain watershed that can be calculated by the infiltration curve or infil-  
 377 tration experiment data. In this study,  $I_m$  has been picked up from Handbook of rainstorm  
 378 and flood in Sichuan (Sichuan Water and Power Department 1984); and  $P_a$  is the antecedent  
 379 precipitation index, referring to the total rainfall prior to the 1-hour peak rainfall leading to  
 380 debris flow initiation.

381 Eq. 5 can be expressed as follows:

$$382 \quad P + P_a = R + I_m \quad (4)$$

383 The precipitation intensity is a measure of the peak precipitation. At the same time, the  
 384 duration of the peak precipitation is generally brief, lasting only up to tens of minutes. There-  
 385 fore, 10-minute precipitation intensity (maximum precipitation over a 10-minute period dur-  
 386 ing the rainfall event) is selected as the stimulating rainfall for debris flow, which is appropri-  
 387 ate and most representative. However, it is difficult to obtain such short-duration rainfall data  
 388 in areas with scarcity of data. Therefore, in this study,  $P$  and  $P_a$  are replaced by  $I_{60}$  (1 hour  
 389 rainfall) and  $API$  (the antecedent precipitation index), respectively; thus, Eq. 6 is expressed  
 390 as:

$$391 \quad I_{60} + API = R + I_m \quad (5)$$

392 In the hydrological study, the runoff depth  $R$  is:

$$393 \quad R = \frac{W}{1000F} = \frac{3.6 \sum Q \cdot \Delta t}{F} = \frac{3.6Q}{F} \quad (6)$$

394 where  $R$  is the runoff depth (m);  $W$  is the total volume of runoff (m<sup>3</sup>);  $F$  is the watershed area  
 395 (km<sup>2</sup>);  $\Delta t$  is the duration time, in this study it is 1 hour; and  $Q$  is the average flow of the water-  
 396 shed (m<sup>3</sup>/s), which can be expressed as follows:

$$397 \quad Q = BVh_0 \quad (7)$$

398 where  $B$  is the width of the channel (m),  $V$  is the average velocity (m/s) and  $h_0$  is the critical  
 399 depth (m).

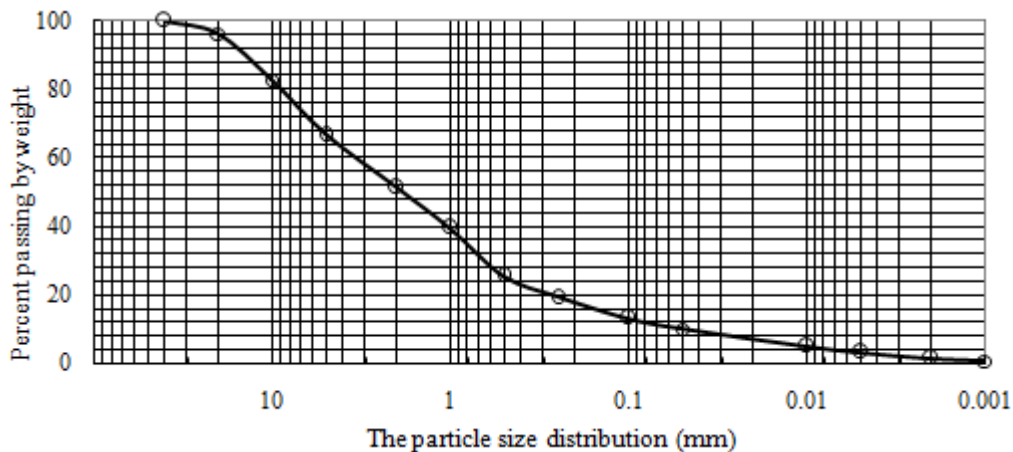
400 Eq. 5 is the expression of the rainfall threshold curve for a watershed, which can be used  
 401 for debris flow early warning. This proposed rainfall threshold curve is a function of the ante-  
 402 cedent precipitation index ( $API$ ) and 1-hour rainfall ( $I_{60}$ ), which is a line and a negative  
 403 slope.

#### 404 4 Results

##### 405 4.1 The rainfall threshold curve of debris flow

###### 406 4.1.1 The critical depth of the Guojuanyan gully

407 The grain grading graph (Fig. 11) is obtained by laboratory grain size analysis experi-  
 408 ments for the loose deposits of the Guojuanyan gully. Figure 11 shows that the characteristic  
 409 particle sizes  $d_{16}$ ,  $d_{50}$ ,  $d_{84}$  and  $d_m$  are 0.18 mm, 1.9 mm, and 10.2 mm, 4.1 mm, respective-  
 410 ly. According to Eq. (1), the critical depth ( $h_0$ ) of the Guojuanyan gully is 7.04 mm.



411  
 412 **Figure 11.** The grain grading graph of the Guojuanyan gully

413 **Table 4.** Critical water depth of debris flow triggering in Guojuanyan gully

$C_*$	$\sigma$ (g/cm <sup>3</sup> )	$\rho$ (g/cm <sup>3</sup> )	$\theta$ (°)	$\tan \theta$	$d_{16}$ (mm)	$d_{50}$ (mm)	$d_{84}$ (mm)	$d_m$ (mm)	$\phi$ (°)	$\tan \phi$	$h_0$ (mm)
0.812	2.67	1.0	18.42	0.333	0.18	1.9	10.2	4.1	21.21	0.388	7.04

###### 414 4.1.2 The rainfall threshold curve of debris flow

415 Taking the cross-section at the outlet of the debris flow formation region as the computa-  
 416 tion object, based on the field investigations and measurements, the width of the cross-section  
 417 is 20 m, and the average velocity of debris flows which is calculated by the several debris flow  
 418 events, is 1.5m/s. Based on the Handbook of rainstorm and flood in Sichuan (Sichuan Water  
 419 and Power Department 1984), the watershed maximum storage capacity ( $I_m$ ) of the  
 420 Guojuanyan gully is 100mm. According to Eq. (5) - Eq. (7), the calculated rainfall threshold  
 421 curve of debris flow in the Guojuanyan gully is shown in Table 5.

422 **Table 5.** The calculated process of the rainfall threshold

Watershed	$h_0$ (mm)	$B$ (m)	$V$ (m/s)	$Q$ (m <sup>3</sup> /s)	$\Delta t$ (h)	$F$ (km <sup>2</sup> )	$R$ (mm)	$I_m$ (mm)	$R + I_m$ (mm)
Guojuanyan	7.04	20.0	1.5	0.197	1	0.11	6.9	100	106.9

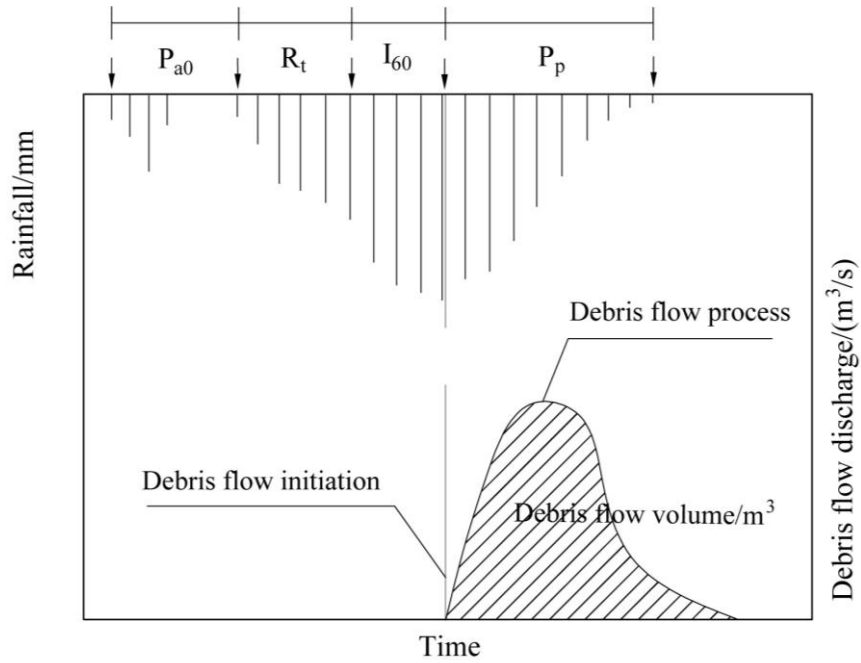
423 From the calculated results, we can conclude the rainfall threshold of the debris flow is  
 424  $I_{60} + API = R + I_m = 106.9 \approx 107$  mm; that is, when the sum of the antecedent precipitation in-  
 425 dex ( $API$ ) and the 1 hour rainfall ( $I_{60}$ ) reaches 107 mm (early warning area), the gully may  
 426 trigger debris flow.

## 427 **4.2 Validation of the results**

### 428 **4.2.1 The calculation of the antecedent precipitation index ( $API$ )**

429 The rainfall factor influencing debris flows consists of three parts: indirect antecedent  
 430 precipitation (IAP) (it is  $P_{a0}$  in this paper), direct antecedent precipitation (DAP) (it is  $R_t$  in this  
 431 paper), and triggering precipitation (TP) (it is  $I_{60}$  in this paper). The relationships among them  
 432 are shown in Figure 12. Obviously, IAP increases soil moisture and decreases the soil stability,  
 433 and DAP saturates soils and thus decrease the critical condition of debris flow occurrence.  
 434 Although TP is believed to initiate debris flows directly, its contribution amounts to only 37%  
 435 of total water (Cui et al. 2007). Guo et al (2013) analyzed the rainstorms and debris flow  
 436 events during June and September in 2006 and 2008, there were 208 days with antecedent  
 437 rainfall more than 10mm, approximately 57% days of the rain season. Among them, there  
 438 were 66 days with antecedent rainfall between 10-15mm, and 1 debris flow event happened;

439 53 days between 15-20 mm and 4 debris flow events happened; 28 days between 20-25 mm  
 440 and 4 debris flow events happened; 30 days between 25-33 mm and 5 debris flow happened;  
 441 and 35 days more than 33mm and 9 debris flow events happened. So, this group of data can  
 442 specifically illustrate the importance of the antecedent rainfall to the debris flow events.



443  
 444

Figure 12. Rainfall index classifications

445 As Fig. 12 shows, take 1-h rainfall ( $I_{60}$ ) that obtained from the observed data of the  
 446 Guojuanyan gully for the TP. The antecedent precipitation index ( $API$ ) includes IAP and  
 447 DAP, calculated as the following expression (Zhao, 2011; Guo, 2013; Zhuang, 2015):

$$448 \quad API = P_{a0} + R_t \quad (8)$$

449 where  $P_{a0}$  is the effective antecedent precipitation (mm) and  $R_t$  is the direct antecedent precip-  
 450 itation (mm), which is the precipitation from the beginning of the rainfall that trigger debris  
 451 flow to the 1 hour before the debris flow.

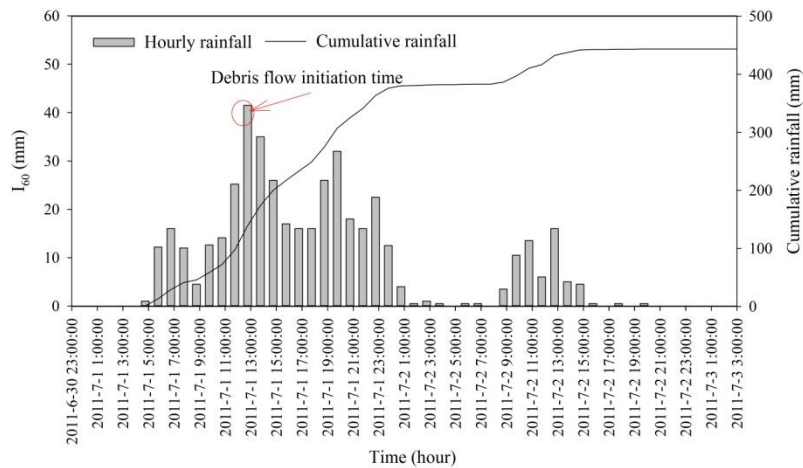
452 It's difficult to study the influence of antecedent rainfall to debris flow as it mainly relies  
 453 on the heterogeneity of soils (strength and permeability properties), which makes it hard to  
 454 measure the moisture. Usually, the frequently used method for calculating antecedent daily  
 455 rainfall is the weighted sum equation as below (Crozier and Eyles 1980; Glade et al. 2000):

$$456 \quad P_{a0} = \sum_1^n P_i \cdot K_i \quad (9)$$

457 Where  $P_i$  is the daily precipitation in the  $i$ -th day proceeding to the debris flow event

458  $(1 \leq i \leq n)$  and  $K_i$  is a decay coefficient due to evaporation and geomorphological condi-  
 459 tions of the soil. The value of the  $K$  can be determined by the test of soil moisture content  
 460 based on Eq.9 in the watershed. The effect of a rainfall event usually diminishes with the time  
 461 going forward. Different patterns of storm debris flow gullies require different numbers of  
 462 previous indirect rainfall days, which can be determined by the relationship between the  
 463 stimulating rainfall and the antecedent rainfall of a debris flow (Pan, et al., 2013). If the rain-  
 464 fall is sharp and heavy, the initiation of debris flow would mainly be determined by DAP and  
 465 TP, while the influence of the antecedent precipitation would be decreased, and vice versa.  
 466 Generally, a typical rainstorm debris flow gully requires no more than 20 days of antecedent  
 467 rainfall.

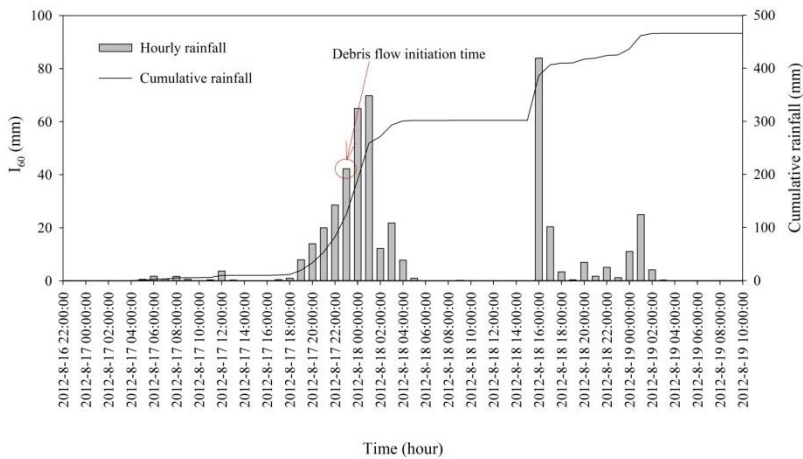
468 **4.2.2 The rainstorm and debris flow events in the Guojuanyan gully during**  
 469 **2010-2014**



470

471

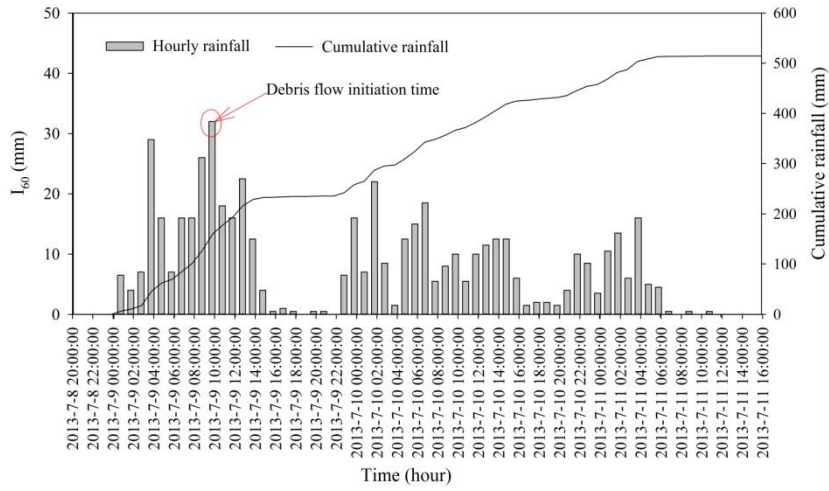
(a)



472

473

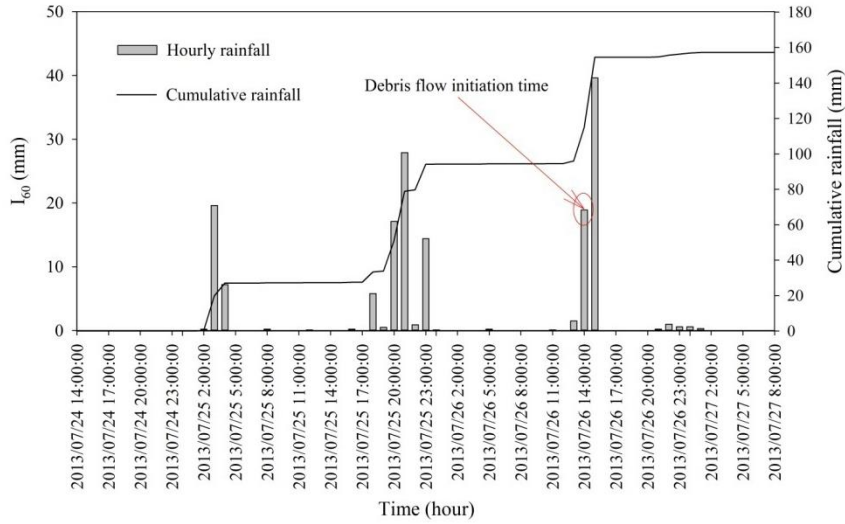
(b)



474

475

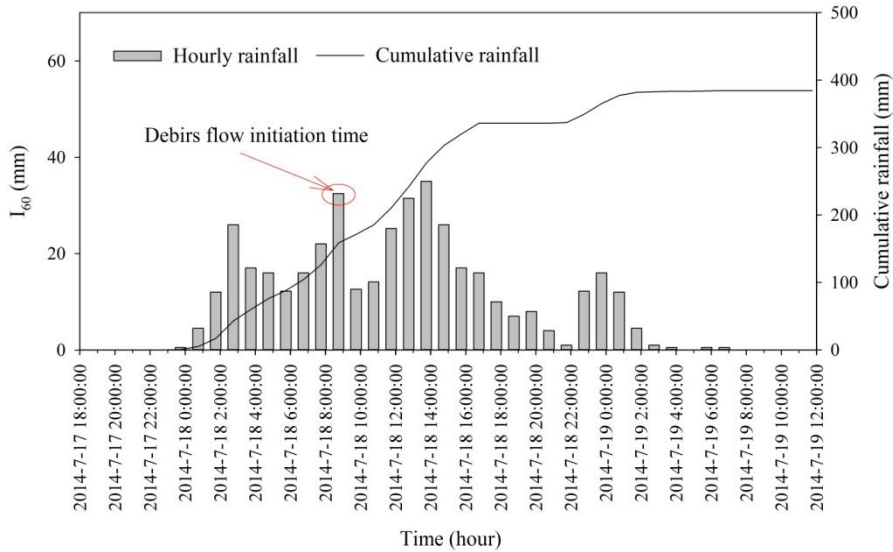
(c)



476

477

(d)



478

479

(e)

480 **Figure 13.** The rainfall process of debris flow vents in the Guojuanyan gully from 2011 to 2014 (a, July  
481 1, 2011; b, August 17, 2012; c, July 9, 2013; d, July 26, 2013; e, July 18, 2014)

482 Table 3 shows that debris flows occurred almost every year after the earthquake. Based  
483 on the field tests and experience, the value of  $K$  and  $n$  in Eq.9 are identified as 0.8 and 20  
484 days separately (Cui et al. 2007). Thus, the duration and intensity of the 1-h triggering rain-  
485 fall and cumulative rainfall for the typical rainstorms are shown in Table 6.

486 In addition to the rainfall process of the 5 debris flow events (Fig. 13), some typical rain-  
487 falls whose daily rainfall were greater than 50 mm but did not trigger a debris flow were also  
488 calculated; the greatest 1-h rainfall is considered as  $I_{60}$  (Table 6).

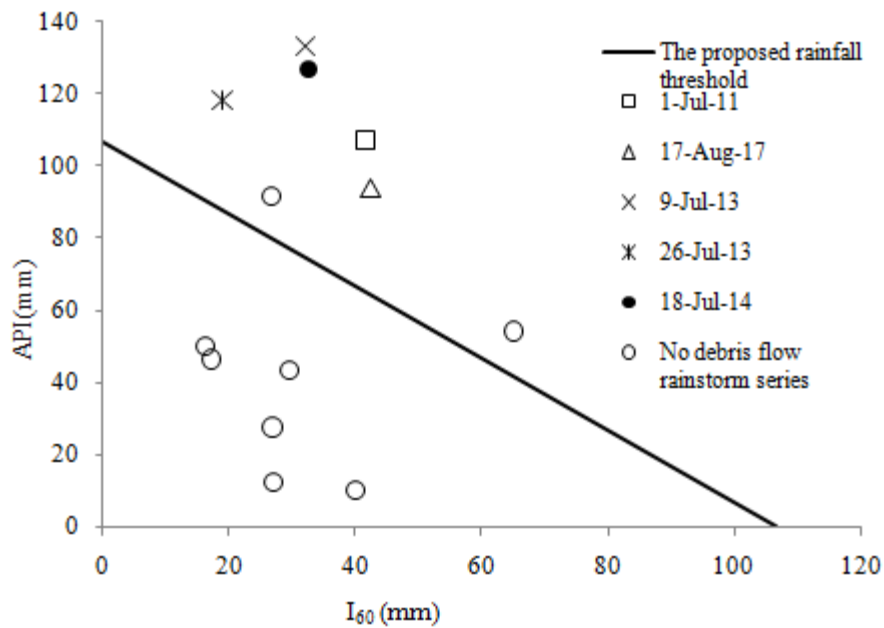
489 **Table 6.** The data of typical rainfall in the Guojuanyan gully after the earthquake

Time	Daily rainfall (mm)	$Pa_0$ (mm)	$R_t$ (mm)	$API$ (mm)	$I_{60}$ (mm)	$API+I_{60}$ (mm)	Location to the threshold line	Triggered debris flow
1 July, 2011		9.7	97.6	107.3	41.5	148.8	Above	Yes
17 August , 2012		12.1	81.9	94.0	42.3	136.3	Above	Yes
9 July , 2013		5.7	127.5	133.2	32	165.2	Above	Yes
26 July , 2013		22.4	96.0	118.4	18.9	137.3	Above	Yes
18 July, 2014		10.7	116.2	126.9	32.5	159.4	Above	Yes
20 August , 2011	82.8	8.5	19.0	27.5	26.8	54.3	Below	No
5 September , 2011	52.1	48.7	1.2	49.9	16.2	66.1	Below	No
16 June , 2012	55.8	5.6	6.6	12.2	27.0	39.2	Below	No
3 August , 2012	148.3	7.5	84.3	91.8	26.7	118.5	Above	No
18 August , 2012	125.7	54.3	0	54.3	65.0	119.3	Above	No
18 June , 2013	50.6	6.2	3.8	10.0	40.0	50.0	Below	No
28 July , 2013	59.4	13.4	30.0	43.4	29.4	72.8	Below	No
6 August , 2013	56.1	12.4	34.0	46.4	17.1	63.5	Below	No

490

491 The proposed rainfall threshold curve is a function of the antecedent precipitation index  
492 ( $API$ ) and 1-h rainfall ( $I_{60}$ ), which is a line and a negative slope. Fig. 14 shows that the calcu-  
493 lated values  $I_{60} + API$  of debris flow events in the Guojuanyan gully are all above the rainfall  
494 threshold curve, while most of the rainstorms that did not trigger debris flow are lay below the  
495 curve. That is, the proposed rainfall threshold curve is reasonable through the validation by  
496 rainfall and hazards data of the Guojuanyan gully.

497



498  
499

**Figure 14.** The proposed rainfall threshold curve of debris flow in the Guojuanyan gully

## 500 5 Discussions

### 501 5.1 About the two above points that did not trigger debris flows

502 The proposed rainfall threshold curve is a function of the antecedent precipitation index  
 503 ( $API$ ) and the 1-h rainfall ( $I_{60}$ ), which has been validated by rainfall and hazards data and  
 504 can be applied to debris flow early warning and mitigation. However, in Figure 14, there are  
 505 two points above the curve that did not trigger debris flow at all. Although we have highlight-  
 506 ed the significance and interconnect of antecedent rainfall, critical rainfall, 1 h triggering  
 507 rainfall, as well as their accurate determination before the hour of debris flow triggering, it  
 508 should be noticed that the rainfall is only the triggering factor of debris flows. A comprehen-  
 509 sive warning system must contain more environmental factors, such as the geologic and geo-  
 510 morphologic factors, the distribution of source areas. The special and complex formative en-  
 511 vironment of debris flow after earthquake caused the rainfall threshold is much more complex  
 512 and uncertain. The rainfall threshold of debris flow varies with the antecedent precipitation  
 513 index ( $API$ ), rainfall characteristics, amount of loose deposits, channel and slope characteris-  
 514 tics, and so on. Therefore, we should further study the characteristics of the movable solid  
 515 materials, the shape of gully, and so on to modify the rainfall threshold curve.

516 On the other hand, restricted by the limited rainfall data, this study was validated by only



517 5 debris flow events. Furthermore, as the initiation depth in distinct watershed is different  
518 from each other because of the different topography and loose solid materials, hence the rain-  
519 fall threshold is independent for each watershed. While most of debris flow gullies in Wen-  
520 chuan earthquake affected areas with scarcity of rainfall data and disaster data, therefore, the  
521 approach proposed in this study hasn't been validated by other gullies except the Guojuanyan  
522 gully so far. Figure 13 and Figure 14 indicated that the only 5 debris flow events all triggered  
523 by the rainfalls with high-intensity and short-duration. As mentioned before, the influence of  
524 the antecedent rainfall in this kind of debris flow is relatively less. However, it still can't ignore  
525 the significance role of the antecedent precipitation. Due to safety concerns, in the universali-  
526 ty calculation of rainfall threshold for debris flow, it must fully consider the antecedent pre-  
527 cipitation. Therefore, the days count for antecedent rainfall in this study is selected as 20. Of  
528 course, the value of the curve should be further validated and continuously corrected with  
529 more rainfall and disaster data in later years.

## 530 **5.2 Further studies about the debris flow early warning in earthquake-hit** 531 **areas**

532 It should be noted that the methodological proposal of this study is based on the physical  
533 process of debris flow initiation and involves modeling with physical characteristics of the  
534 loose solid materials which served by the landslides triggered by earthquake; therefore, it's  
535 suitable for the areas with scarcity of data especially the earthquake affected areas.

536 Actually, the times of debris flow events happened in the earthquake-hit areas were de-  
537 creasing from 2014 on; there was even no debris flow event at all in Guojuanyan gully. Mainly  
538 because of the unstable slopes as well as the materials are decreasing with the times go by.  
539 Therefore, the rainfall threshold would increase accordingly. However, it may need a long  
540 time, perhaps 15-20 years, according to the experiences in other earthquake-hit areas, such as  
541 Chi-Chi earthquake, to recover to the normal value. Hence, the rainfall threshold is not a con-  
542 stant value but changing with time.

## 543 **6 Conclusions**

544 (1) In the Wenchuan earthquake-stricken areas, loose deposits are widely distributed,

545 causing dramatic changes on the environmental development for the occurrence of debris  
546 flow; thus, the debris flow occurrence increased dramatically in the subsequent years. The  
547 characteristics of the 10-min, 1-h and 24-h critical rainfalls were represented based on a com-  
548 prehensive analysis of limited rainfall and hazards data. The statistical results show that the  
549 10-min and 1-h critical rainfalls of different debris flow events have minor differences; how-  
550 ever, the 24 hour critical rainfalls vary widely. The 10-min and 1-h critical rainfalls have a no-  
551 tably higher correlation with debris flow occurrences than to the 24-h critical rainfalls.

552 (2) The rainfall pattern of the Guojuanyan gully is the peak pattern, both single peak and  
553 multi-peak. The antecedent precipitation index (*API*) was fully explored by the antecedent  
554 effective rainfall and stimulating rainfall.

555 (3) As an important and effective means of debris flow early warning and mitigation, the  
556 rainfall threshold of debris flow was determined in this paper, and a new method to calculate  
557 the rainfall threshold is put forward. Firstly, the rainfall characteristics, hydrological charac-  
558 teristics, and some other topography conditions were analysed. Then, the critical water depth  
559 for the initiation of debris flows is calculated according to the topography conditions and  
560 physical characteristics of the loose solid materials. Finally, according to the initiation mecha-  
561 nism of hydraulic-driven debris flow, combined with the runoff yield and concentration laws  
562 of the watershed, this study promoted a new method to calculate the debris flow rainfall  
563 threshold. At last, the hydrological condition for the initiation of a debris flow is the result of  
564 both short-duration heavy rains ( $I_{60}$ ) and the antecedent precipitation index (*API*). The  
565 proposed approach resolves the problem of debris flow early warning in areas with scarcity  
566 data, can be used to establish warning systems of debris flows for similar catchments in areas  
567 with scarcity data although it still need further modification. This study provides a new  
568 thinking for the debris flow early warning in the mountain areas.

## 569 **Acknowledgments**

570 This paper is supported by the CRSRI Open Research Program (Program No:  
571 CKWV2015229/KY), CAS Pioneer Hundred Talents Program, and National Nature Science  
572 Foundation of China (No. 41372331 & No. 41672318).

573 **References**

- 574 Bai LP, Sun JL, Nan Y (2008) Analysis of the critical rainfall thresholds for mudflow in Beijing, China. *Geological*  
575 *Bulletin of China* 27(5): 674-680. (in Chinese)
- 576 Baum RL, Godt JW (2010). Early warning of rainfall-induced shallow landslides and debris flows in the USA.  
577 *Landslides*, 7(3):259–272.
- 578 Caine, N (1980) The rainfall intensity-duration control of shallow landslides and debris flows. *Physical Geography*  
579 62A (1-2):23-27
- 580 Campbell RH (1975) Debris Flow Originating from Soil Slip during Rainstorm in Southern California. *Q. Engineering*  
581 *Geologist* 7: 339–349. DOI:10.1144/GSL.QJEG.1974.007.04.04
- 582 Cannon, Susan H., et al. (2008) Storm rainfall conditions for floods and debris flows from recently burned areas in  
583 southwestern Colorado and southern California. *Geomorphology* 96(3): 250-269.
- 584 Chen, Su-Chin, and Bo-Tsung Huang (2010) Non-structural mitigation programs for sediment-related disasters after  
585 the Chichi Earthquake in Taiwan. *Journal of Mountain Science* 7(3): 291-300.
- 586 Chen YS (2008) An influence of earthquake on the occurrence of landslide and debris flow. Taipei: National Cheng  
587 Kung University.
- 588 Chen YJ, Yu B, Zhu Y, et al. (2013) Characteristics of critical rainfall of debris flow after earthquake - a case study of  
589 the Xiaogangjian gully. *Journal of Mountain Science* 31(3): 356-361. (in Chinese)
- 590 Cheng ZL, Zhu PY, Liu LJ (1998) The Relationship between Debris Flow Activity and Rainfall Intensity. *Journal of*  
591 *Natural Disasters* 7 (1): 118–120. (in Chinese)
- 592 Chen NS, Yang CL, Zhou W, et al. (2009) The Critical Rainfall Characteristics for Torrents and Debris Flows in the  
593 Wenchuan Earthquake Stricken Area. *Journal of Mountain Science* 6: 362-372. DOI: 10.1007/s11629-009-1064-9
- 594 Cui P (1991) Experiment Research of the Initial Condition and Mechanism of Debris Flow. *Chinese Science Bulletin*  
595 21:1650–1652. (in Chinese)
- 596 Cui P, Hu KH, Zhuang JQ, Yang Y, Zhang J (2011) Prediction of debris-flow danger area by combining hydro-logical  
597 and inundation simulation methods. *Journal of Mountain Science* 8(1): 1-9. doi: 10.1007/s11629-011-2040-8
- 598 Cui P, Zhu YY, Chen J, et al. (2007) Relationships between antecedent rainfall and debris flows in Jiangjia Ravine,  
599 China. In: Chen C L and Majir JJ (eds.), *Debris flow hazard mitigation mechanics, Prediction, and Assessment*.  
600 Millpress, Rotterdam: 1-10.
- 601 Dahal RK, Hasegawa S, Nonomura A, et al. (2009) Failure characteristics of rainfall-induced shallow landslides in  
602 granitic terrains of Shikoku Island of Japan. *Environmental geology* 56(7): 1295-1310. DOI:  
603 10.1007/s00254-008-1228-x
- 604 Degetto M, Gregoretti C, Bernard M (2015) Comparative analysis of the differences between using LiDAR  
605 contour-based DEMs for hydrological modeling of runoff generating debris flows in the Dolomites. *Front. Earth Sci.*  
606 3, 21. doi: 10.3389/feart.2015.00021
- 607 Gregoretti C, Degetto M, Boreggio M (2016) GIS-based cell model for simulating debris flow runout on a fan. *Journal*  
608 *of Hydrology* 534: 326-340. doi: 10.1016/j.jhydrol.2015.12.054
- 609 Guido Rianna, Luca Pagano, Gianfranco Urciuoli (2014) Rainfall patterns triggering shallow flowslides in pyroclastic

610 soils. *Engineering Geology*, 174: 22-35 doi: 10.1016/j.enggeo.2014.03.004

611 Guo, X.J., Cui, P., Li, Y., 2013. Debris flow warning threshold based on antecedent rainfall: a case study in Jiangjia  
612 Ravine, Yunnan, China. *J. Mt. Sci.* 10 (2), 305–314.

613 Guzzetti, F., Peruccacci, S., Rossi, M., & Stark, C. P. (2008). The rainfall intensity–duration control of shallow  
614 landslides and debris flows: an update. *Landslides*, 5(1), 3-17.

615 Hu M J, Wang R (2003) Testing Study of the Correlation among Landslide, Debris Flow and Rainfall in Jiangjia Gully.  
616 *Chinese Journal of Rock Mechanics and Engineering*, 22(5): 824–828 (in Chinese)

617 Hong Y, Hiura H, Shino K, et al. (2005) The influence of intense rainfall on the activity of large-scale crystalline schist  
618 landslides in Shikoku Island, Japan. *Landslides* 2(2): 97-105. DOI: 10.1007/s10346-004-0043-z

619 Hu W, Dong XJ, Wang GH, van Asch TWJ, Hicher PY (2016) Initiation processes for run-off generated debris flows  
620 in the Wenchuan earthquake area of China. *Geomorphology* 253: 468–477. doi: 10.1016/j.geomorph.2015.10.024

621 Iverson RM, Lahusen RG (1989) Dynamic Pore-Pressure Fluctuations in Rapidly Shearing Granular Materials.  
622 *Science* 246 (4931): 796–799. DOI: 10.1126/science.246.4931.796

623 Jianqi Zhuang, Peng Cui, Gonghui Wang, et al. (2015) Rainfall thresholds for the occurrence of debris flows in the  
624 Jiangjia Gully, Yunnan Province, China. *Engineering Geology*, 195: 335-346.

625 Jibson RW (1989) Debris flows in southern Puerto Rico. *Geological Society of America Special Papers* 236: 29-56.  
626 DOI: 10.1130/SPE236-p29

627 Jun Wang, Shun Yang, Guoqiang Ou, et al. (2017) Debris flow hazards assessment by combing numerical simulation  
628 and land utilization. *Bulletin of Engineering Geology and the Environment*, 1-15. Doi: 10.1007/s10064-017-1006-7.

629 Liang GM, Yao LK (2008) Study on the critical rainfall for debris flows. *Lu Ji Gongcheng* 6: 3-5. (in Chinese)

630 Liu YH, Tang C, Li TF, et al. (2009) Statistical relations between geo-hazards and rain type. *Journal of Engineering*  
631 *Geology* 17(5): 656-661. (in Chinese)

632 Liu JF, You Y, Chen XZ, Fan JR (2010) Identification of potential sites of debris flows in the upper Min River  
633 drainage, following environmental changes caused by the Wenchuan earthquake. *Journal of Mountain Science* 3:  
634 255-263. doi: 10.1007/s11629-010-2017-z

635 Lanzoni, S., C. Gregoretti, and L. M. Stancanelli (2017), Coarse-grained debris flow dynamics on erodible beds, *J.*  
636 *Geophys. Res. Earth Surf.*, 122, doi:10.1002/2016JF004046.

637 McCoy SW, Kean JW, Coe JA, Tucker GE, Staley DM, Wasklewicz WA (2012) Sediment entrainment by debris flows:  
638 In situ measurements from the head waters of a steep catchment. *J. Geophys. Res.* 117, F03016. doi:  
639 10.1029/2011JF002278

640 Mohamad Ayob Mohamadi, Ataollah Kaviani (2015) Effects of rainfall patterns on runoff and soil erosion in field plots.  
641 *International Soil and Water Conservation Research* 3: 273-281.  
642 <http://dx.doi.org/10.1016/j.iswcr.2015.10.001>

643 Imaizumi F, Sidle RC, Tsuchiya S, Ohsaka O (2006)  
644 Hydrogeomorphic processes in a steep debris flow initiation zone. *Geophys. Res. Lett.* 33, L10404. doi:  
10.1029/2006GL026250

645 Pan HL, Ou GQ, Hang JC, et al. (2012) Study of rainfall threshold of debris flow forewarning in data lack areas. *Rock*  
646 *and Soil Mechanics* 33(7): 2122-2126. (in Chinese)

647 Pan HL, Huang JC, Wang R, et al. (2013) Rainfall Threshold Calculation Method for Debris Flow Pre-Warning in  
648 Data-Poor Areas. *Journal of Earth Science* 24(5): 854–862. DOI:10.1007/s12583-013-0377-3

649 Rosi A, Lagomarsino D, Rossi G, Segoni S, Battistini A, Casagli N (2015) Updating EWS rainfall thresholds for the  
650 triggering of landslides. *Nature Hazard* 78:297–308

651 Saito H, Nakayama D, Matsuyama H (2010) Relationship between the initiation of a shallow landslide and rainfall  
652 intensity–duration thresholds in Japan. *Geomorphology* 118(1): 167-175. DOI:  
653 10.1016/j.geomorph.2009.12.016

654 Segoni S, Battistini A, Rossi G, Rosi A, Lagomarsino D, Catani F, Moretti S,  
655 Casagli N (2015) Technical note: an operational landslide early warning system at regional scale based on  
656 space–time variable rainfall thresholds. *Nat Hazards Earth Syst Sci* 15: 853–861

657 Shied CL, Chen LZ (1995) Developing the critical line of debris –flow occurrence. *Journal of Chinese Soil and Water  
658 Conservation* 26(3):167-172. (in Chinese)

659 Shieh CL, Chen YS, Tsai YJ, et al (2009) Variability in rainfall threshold for debris flow after the Chi-Chi earthquake  
660 in central Taiwan, China. *International Journal of Sediment Research* 24(2): 177-188.

661 Staley, D.M., Kean, J.W., Cannon, S.C., Schmidt, K.M., Laber, J.L. (2013) Objective definition of rainfall  
662 intensity–duration thresholds for the initiation of post-fire debris flows in southern California, *Landslides* 10,  
663 547–562

664 Takahashi T (1978) Mechanical Characteristics of Debris Flow. *Journal of the Hydraulics Division* 104:1153–1169

665 Tang C, Zhu J, Li WL (2009) Rainfall-triggered debris flows following the Wenchuan earthquake. *Bull Eng Geol  
666 Environ* 68(2):187–194. DOI: 10.1007/s10064-009-0201-6

667 Tang C, Van Asch TWJ, Chang M, et al.(2012) Catastrophic debris flows on 13 August 2010 in the Qingping area,  
668 southwestern China: the combined effects of an earthquake and subsequent rainstorms.  
669 *Geomorphology* 139–140:559–576. DOI: 10.1016/j.geomorph.2011.12.021

670 Tang C, Zhu J, Chang M, et al. (2012) An empirical–statistical model for predicting debris-flow runout zones in the  
671 Wenchuan earthquake area. *Quaternary International* 250:63–73. DOI:10.1016/j.quaint.2010.11.020.

672 Tecca PR, Genevois R (2009) Field observations of the June 30, 2001 debris flow at Acquabona (Dolomites, Italy).  
673 *Landslides* 6(1): 39-45. doi: 10.1007/s10346-009-0145-8

674 Tian B, Wang YY, Hong Y (2008) Weighted relation between antecedent rainfall and process precipitation in debris  
675 flow prediction—A case study of Jiangjia gully in Yunnan province. *Bulletin of Soil and Water Conservation* 28(2):  
676 71-75.(in Chinese)

677 Tiranti D, Deangeli C (2015) Modeling of debris flow depositional patterns according to the catchment and sediment  
678 source area characteristics. *Front. Earth Sci.* 3, 8. doi: 10.3389/feart.2015.00008

679 Tofani et al., Soil characterization for shallow landslides modeling: a case study in the Northern Apennines (Central  
680 Italy). 2017. *Landslides* 14:755–770, DOI 10.1007/s10346-017-0809-8

681 Y.Zhao, F. Wei, H.Yang, et al. (2011) Discussion on Using Antecedent Precipitation Index to Supplement Relative Soil  
682 Moisture Data Series. *Procedia Environment Sciences* 10: 1489-1495.

683 Wang EC, Meng QR (2009) Mesozoic and cenozoic tectonic evolution of the Longmenshan fault belt. *Science in China  
684 Series D: Earth Sciences* 52(5): 579-592. DOI:10.1007/s11430-009-0053-8

685 Wang J, Ou GQ, Yang S, Lu GH, et al. (2013) Applicability of geomorphic information entropy in the post-earthquake

685 debris flow risk assessment. *Journal of Mountain Science* 31(1): 83-91. (in Chinese)

686 Wang J, Yu Y, Yang S, et al.(2014) A Modified Certainty Coefficient Method (M-CF) for Debris Flow Susceptibility  
687 Assessment: A Case Study for the Wenchuan Earthquake Meizoseismal Areas. *Journal of Mountain Science*11(5):  
688 1286-1297. DOI: 10.1007/s11629-013-2781-7.

689 Wang J, Yu Y, Ou GQ, et al.(2016) Study on the Geotechnical Mechanical Characteristics of Loose Materials in the  
690 Wenchuan Earthquake-hit Areas. *Science Technology and Engineering* 16(5): 11-18. (in Chinese)

691 Wieczorek GF (1987) Effect of rainfall intensity and duration on debris flows in central Santa Cruz Mountain, California.  
692 *Engineering Geology* 7: 93-104. DOI: 10.1130/REG7-p93

693 Wilson, RC, Jayko AS (1997) Preliminary Maps Showing Rainfall Thresholds for Debris-Flow Activity, San  
694 Francisco Region, California. U.S. Geological Survey Open-File Report 97-745 F

695 Winter, M. G., et al. (2010) Debris flow, rainfall and climate change in Scotland. *Quarterly Journal of Engineering  
696 Geology and Hydrogeology* 43(4): 429-446.

697 Xu ZQ, Ji SC, Li HB, et al. (2008) Uplift of the Longmen Shan range and the Wenchuan earthquake. *Episodes* 31(3):  
698 291-301

699 Xu Q, Zhang S, Li WL, et al.(2012) The 13 August 2010 catastrophic debris flows after the 2008 Wenchuan earthquake,  
700 China. *Natural hazards and earth system sciences* 12(1):201–216. DOI: 10.5194/nhess-12-201-2012

701 Yao LK (1988) A research on the calculation of critical rainfall with frequency of debris flow and torrential rain.  
702 *Journal of Soil and Water Conservation* 2(4): 72-78 (in Chinese)

703 Ye SZ (1992) Hydrological calculation. Water conservancy and Hydropower Press, 111.

704 Zhou, W., & Tang, C. (2014). Rainfall thresholds for debris flow initiation in the Wenchuan earthquake-stricken area,  
705 southwestern China. *Landslides*, 11(5), 877-887.

706 Zhuang JQ, Cui P, Ge YG, et al. (2009) Relationship between rainfall characteristics and total amount of debris flow.  
707 *Journal of Beijing Forestry University* 31(4): 77-83 (in Chinese)

708 Zhang SJ, Yang HJ, Wei FQ, et al. (2014) A Model of Debris Flow Forecast Based on the Water-Soil Coupling  
709 Mechanism. *Journal of Earth Science*, 25(4): 757-763. DOI:10.1007/s12583-014-0463-1

710 Zhenlei Wei, Yuequan Shang, Yu Zhao, et al. (2017) Rainfall threshold for initiation of channelized debris flows in a  
711 small catchment based on in-site measurement. *Engineering Geology*, 217, 23-34.